WORLD JOURNAL OF PHARMACEUTICAL RESEARCH
SJIF Impact Factor 8.074
Volume 7, Issue 6, 23-38. Research Article ISSN 2277– 7105

ULTRA-SENSITIVE SPECTROPHOTOMETRIC DETECTION OF BREAST CANCER THERAPY ANASTROZOLE USING CARBON QUANTUM DOTS/SILVER NANOCOMPOSITE

Abdulkareem Abdulraheem[1], Maha F. El-Tohamy[2]*, Nabeel Alsaffar[3], Maryam Al Hussaini[4]

[1,3,4]Department of Pharmaceutical Sciences, Public Authority for Applied Education and Training, College of Health Sciences, P.O. Box 23167, Safat 13092, Kuwait.

[2]Department of Chemistry, College of Science, King Saud University, P.O. Box 22452, Riyadh 11495, Saudi Arabia.

[2]General Administrative of Medical Affairs, Zagazig University, Egypt.

Article Received on
21 Jan. 2018,
Revised on 11 Feb. 2018,
Accepted on 25 Feb 2018,
DOI: 10.20959/wjpr20186-11382

***Corresponding Author**
Maha F. El-Tohamy
Department of Chemistry, College of Science, King Saud University, P.O. Box 22452, Riyadh 11495, Saudi Arabia.

ABSTRACT

The present study focused on the employment of carbon quantum dots decorated silver nanocomposite (CDQs/Ag) for the detection of breast cancer therapy, anastrozole (ATZ). A green synthesis of glucose-derived CQDs was conducted using a facile microwave-assisted method. Due to the unique interaction of the investigated drug and the as-prepared sensing solution, the color intensities were increased as a function of ATZ concentrations. The suggested method displayed a linear relationship over a concentration range of 5-80 µg mL^{-1} at a wavelength of 224 nm. The lower limit of detection was 2 µg mL^{-1} and the quantification detection limit is 5 µg mL^{-1}. The proposed CQDs/Ag nanocomposite method provides a promising tool for the detection of ATZ in bulk and pharmaceutical formulations.

KEYWORDS: Anastrozole, Carbon Quantum Dots, Silver Nanoparticles, Spectrophotometry, Cancer Therapy.

INTRODUCTION

Cancer is a group of uncontrollable and abnormal growing cells that disregarding the normal rules of cell division and have the potential to invade or spread to other parts of the body.[1] It

is the major cause of death and one of the most striking public health problems worldwide.[2] Breast cancer is the second lethal type of cancer that recognized in women after skin cancer. The early diagnosis and clinical treatment of breast cancer provide a high successful chance for patients survive.

Anastrozole (ATZ) is chemically known as 2-[3(1-cyano-1-methyl-ethyl)-5-(1H-1, 2, 4 triazole-1-yl-methyl) phenyl]-2- methyl-propinenitrile (Figure 1). It is recommended for the treatment of breast cancer in women after menopause.[3]

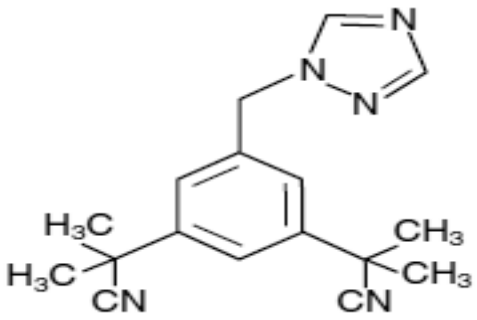

Figure 1: Chemical structure of anastrozole.

Few methods have been reported for the detection of ATZ including HPLC,[4,5] LC/MS,[6] gas chromatography,[7] capillary zone electrophoresis.[8] Furthermore, spectroscopic techniques were addressed for the detection of ATZ such as spectrophotometry.[9]

Recently, nanotechnology is explosively growing and giving infinite benefits in almost our life fields. Among these are medicine,[10] catalysis,[11] drug delivery,[12] drug analysis,[13] tissue engineering,[14] cell imaging,[15] and cancer biomarkers.[16] Moreover, eco-friendly green-synthesized nanoparticles of less hazardous materials to avoid the usage of toxic reagents, reduce the use of chemical reagents and analytical instruments are dramatically increasing as well.[17,18]

Carbon Quantum Dots (CQDs) have unique optical, physicochemical and electronic properties. According to the employed synthesis methodology, it is possible to prepare CQDs with desirable size and specific optical properties.[19]

Several analytical applications such as optoelectronic[20] photocatalysis,[21] photoluminescent,[22] bioimaging and biosensing.[23] Additionally, CQDs have been added as reducing agents in the synthesis of metallic nanocomposites for sensing applications.[24,25]

The present study aimed to develop a simple and ultrasensitive spectrophotometric technique based on CQDs/Ag nanocomposite for the detection of ATZ cancer breast therapy in bulk and pharmaceutical formulations.

EXPERIMENTAL

Instrumentation

UV-vis spectra of CQDs and the nanocomposite were measured using an Ultrospec 2100-Biochrom spectrophotometer, (Biochrom Ltd, Cambium, Cambridge, UK). Transmission electron microscope (TEM) JEOL model 1200EX instrument, (JEOL Ltd, Freising, Germany) was used to evaluate the size and shape of the synthesized CQDs/Ag nanocomposite. X-ray powder diffraction (XRD) pattern was obtained using Siemens D-5000 diffractometer (Siemens, Erfurt, Germany) and Fourier transform infrared (FT-IR) spectra were measured using PerkinElmer FT-IR spectrophotometer (PerkinElmer Ltd, Yokohama, Japan). X-ray photoelectron spectroscopy (XPS).

Chemicals and reagents

Pure grade of ATZ was supplied by Astrazeneca Pharmaceuticals, LP, Wilmington, UK). Anastrozole® 1mg/tablet was purchased from local drug stores Glucose, ammonia (NH_3), methanol and $AgNO_3$ were purchased from (Sigma-Aldrich, Hamburg, Germany). All reagents were of analytical grade. Deionized water obtained from SG-2000-10090 (Barsbuttel, Germany) was used.

Synthesis of CQDs

A simple green synthesis method was used to prepare CQDs (Scheme 1). Approximately; 10 mL of a 15 % aqueous solution of glucose was transferred into a conical flask and heated for 15 min using a conventional microwave 720 W at 120°C. The formation of CQDs was indicated by changing the clear solution into a yellowish transparent semisolid solution (Figure 1a). The obtained volume was completed to 10 mL with deionized water and purified using a dialysis membrane (MW = 2000 Da) against deionized water for 3 h.

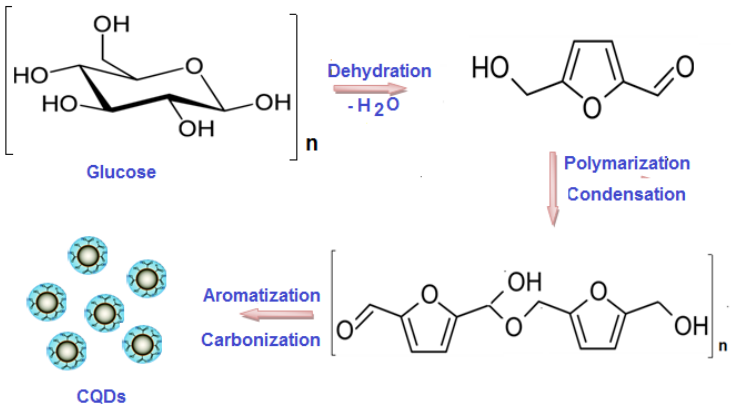

Scheme 1: Steps of thermo dehydration of glucose to form CQDs using microwave-assisted method.

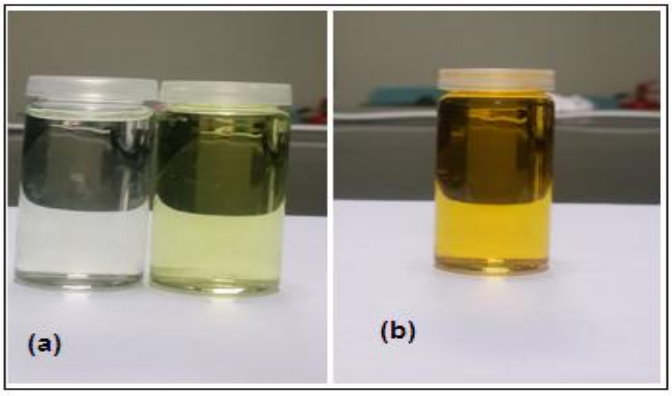

Figure 1: (a) Microwave-assisted method for synthesis of CQDs using glucose and (b) CQDs/Ag nanocomposite.

Preparation of CQDs/Ag nanocomposite

A simple chemical reduction method was used to prepare CQDs/Ag nanocomposite was prepared by adding 5 mL CQDs solution to 3 mL of 1.0×10^{-2} mol L^{-1} of $AgNO_3$ solution and 1.0 mL of 5.0×10^{-2} mol L^{-1} NH_3. The mixture was transferred into a 50-mL conical flask and completed to volume using deionized water. The mixture was then incubated in ambient room temperature for approximately 30 min. A yellow- color solution of CQDs/Ag nanocomposite was obtained and stored in refrigerator for one month at 4º C (Figure 1b).

Preparation of standard drug solution

Standard solution of ATZ 100 µg mL^{-1} was prepared by dissolving 10 mg of the drug into 100 mL methanol. Working solutions in the range of 5-80 µg mL^{-1} were obtained by serial dilutions using the same solvent.

Preparation of Anastrozole tablet solution

Not less than 20 tablets of Anastrozole® tablet 1 mg/tablet were finely powdered and accurate amount equivalent to prepare 100 µg $mL^{-1}$was dissolved in methanol. The solution was centrifuged at 2500 rpm for 3 min. Then, the solution was filtered and serial dilution in the range of 5-80 µg $mL^{-1}$was prepared using methanol as solvent.

General procedure of method detection

The principle of the proposed work is based on the formation of stable CQDs, which have spherical particles with size less than 10 nm and surface active functional moieties. Samples of pure ATZ concentrations of 5-80 µg mL^{-1} were tested. Under optimal conditions, the absorbance intensities were plotted *vs.* the investigated drug concentrations. The calibration graph was plotted and the regression equation was then derived.

RESULTS AND DISCUSSION

Characterization of CQDs

The morphological evaluation of the obtained CQDs was accomplished by TEM. The recorded image revealed mono-dispersed, spherical CQDs with uniform distribution. The high resolution of transmission electron microscope (HRTEM) showed CQDs with sizes less than 10 nm. The calculated particle size distribution curve showed an average particle size of 1.5 - 5 ± 0.1 nm. Dynamic light scattering test (DLS) also confirmed that the average particle size varies between 10 – 26 ± 0.6 nm (Figure 2).

The UV-vis spectrum of CQDs recorded two significant absorption peaks at 224 and 280 nm (Figure 3). These distinct peaks are attributed to the presence of π-π^* transition of C=C and n-π^* transition of the carbonyl group C=O, respectively.

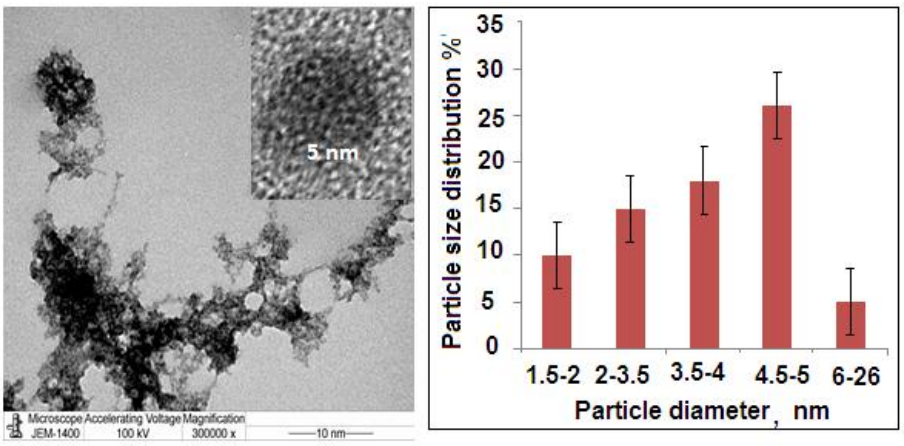

Figure 2: TEM and HRTEM image of CQDs: image of the spherical morphology of mono-dispersed particles with average diameter 5 nm, and particle size distribution curve of CQDs.

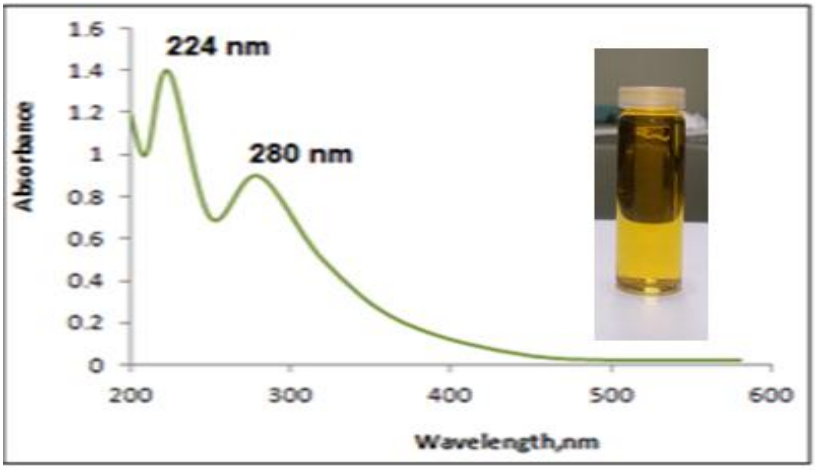

Figure 3: (a) UV-vis absorption spectrum of CQDs.

Characterization of CQD/Ag nanocomposite

Microscopic and spectroscopic techniques were carried out to confirm the characterization of CQDs/Ag nanocomposite. FT-IR spectrum displayed the appearance of different peaks that represent some functional groups which are located on the surface of CQDs such as stretching vibration of C-OH (3300 cm^{-1}) and C-H at (2920 cm^{-1}). Additionally, vibrational absorption bands corresponding to C=O, amide III and C-O-C were recorded at 1750 cm^{-1}, 1381 cm^{-1} and 1250 cm^{-1}, respectively.

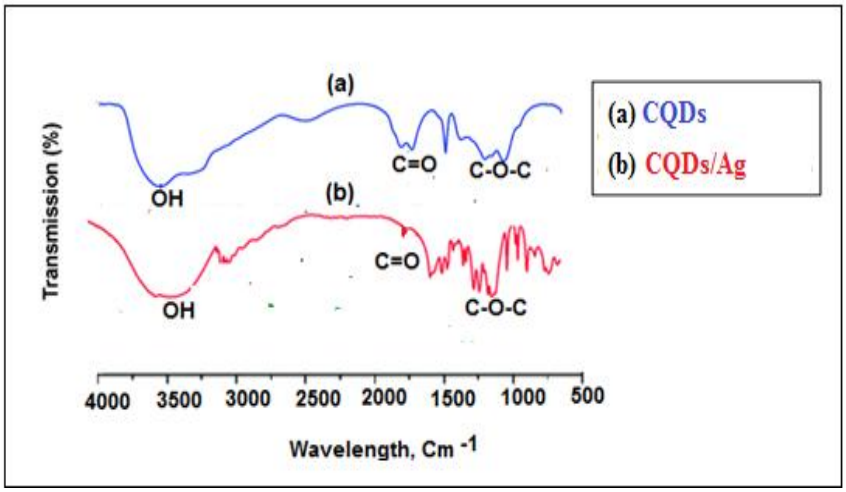

Figure 4: FT-IR Spectra of (a) CQDs and (b) CQDs/Ag nanocomposite.

It worth to mention that the presence of -OH groups with their reducing activity on the surface of CQDs confirmed the ability of CQDs to donate electrons in the formation reaction of CQDs/Ag nanocomposite.

Moreover, the presence of the COOH group on the surface of CQDs, which possess strong affinity towards Ag ions, facilitate the absorption of Ag ions at CQDs surface and prevents their aggregation.

XPS spectrum of CQDs/Ag nanocomposite was recorded and showed that the as-synthesized CQDs/Ag nanocomposite has certain functional groups such as C-C, C-O and C=O with binding energies of 284 eV, 286 eV 289 eV, respectively (Figure 5a). Moreover, two more distinct peaks at binding energies 367 and 373 eV were recorded which are attributed to $Ag3d_{5/2}$ and $Ag3d_{3/2}$, respectively (Figure 5b). Additionally, the high resolution XPS showed the presence of C1s, Ag3d and O1s peaks at binding energies of 284 eV, 370 eV and 530 eV, respectively (Figure 5c). The obtained XPS spectrum confirmed that CQDs surface is decorated by Ag nanoparticles forming CQDs/Ag nanocomposite.

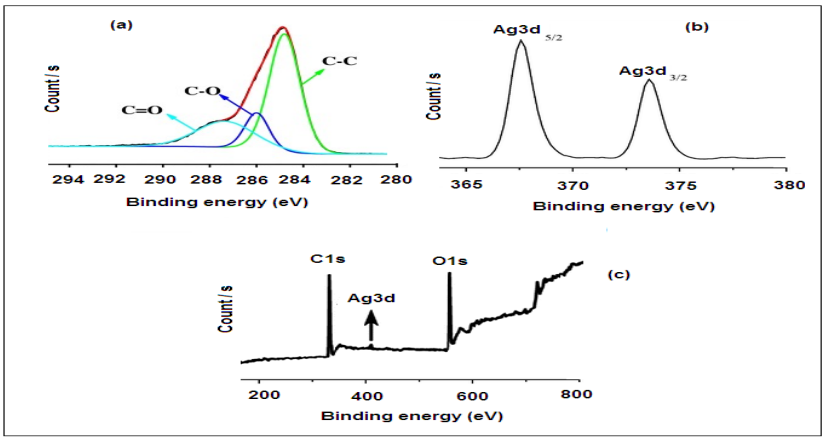

Figure 5: XPS spectra of (a) CQDs, (b) Ag and (c) CQD/Ag nanocomposite.

XRD patterns of CQDs and CQDs/Ag nanocomposite were recorded. It was observed that CQDs in CQDs/Ag nanocomposite is hardly to be distinguished, compared with the XRD pattern of normal CQDs, which exhibits a single broad (002) peak at 19 º (2Θ) can reflect an increase in the interlayer spacing of CQDs as a result of the growth of Ag nanoparticles on the surface of CQDs.[26] In addition, XRD pattern of CQDs/Ag nanocomposite revealed the presence of significantly different peaks at 30º, 38.1º, 64.0º and 77.1º (2Θ), indicating the distribution of Ag (111), Ag (200), Ag (220) and Ag (311), respectively, on CQDs surface.

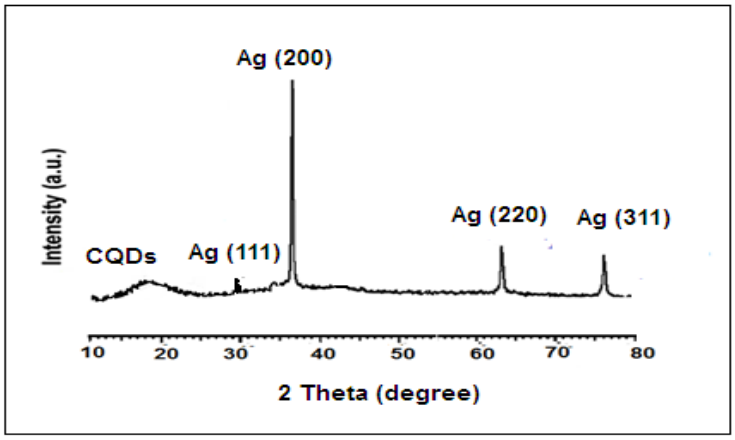

Figure 6: XRD pattern of CQDs/Ag nanocomposite.

Optimization of detection conditions

In order to select the suitable conditions for maximum sensitivity of the proposed technique, various parameters were studied and optimized. The parameters include several experimental variables such as the amount of CQDs/Ag nanocomposite, buffer concentration, pH and reaction time.

The suitable amount of CQDs/Ag nanocomposite was selected by testing different amounts in the range of 0.5 - 4 mL. It was observed that the maximum absorbance was obtained by adding 1.0 mL of CQDs/Ag nanocomposite (Figure 7a).

The absorbance was recorded by varying the pH of universal buffer of 2-7. The peak intensity has slightly changed with changing the pH values. The maximum peak intensity was recorded at pH value 5. (Figure 7b).

The effect of buffer concentration on the peak intensity was investigated using phosphate buffer in a concentration range of 0.2 – 1.0 mol L^{-1} (Figure 7c). The absorbance was elevated by increasing the concentration of buffer up to 0.5 mol L^{-1}. At high buffer concentrations the peak intensity decreased gradually due to the aggregation of CQDs/Ag nanocomposite.

The response time was examined by repeating the analytical process using reaction time in the range of 2-10 min. The suitable time to obtain maximum absorbance was at 5 min (Figure 7d).

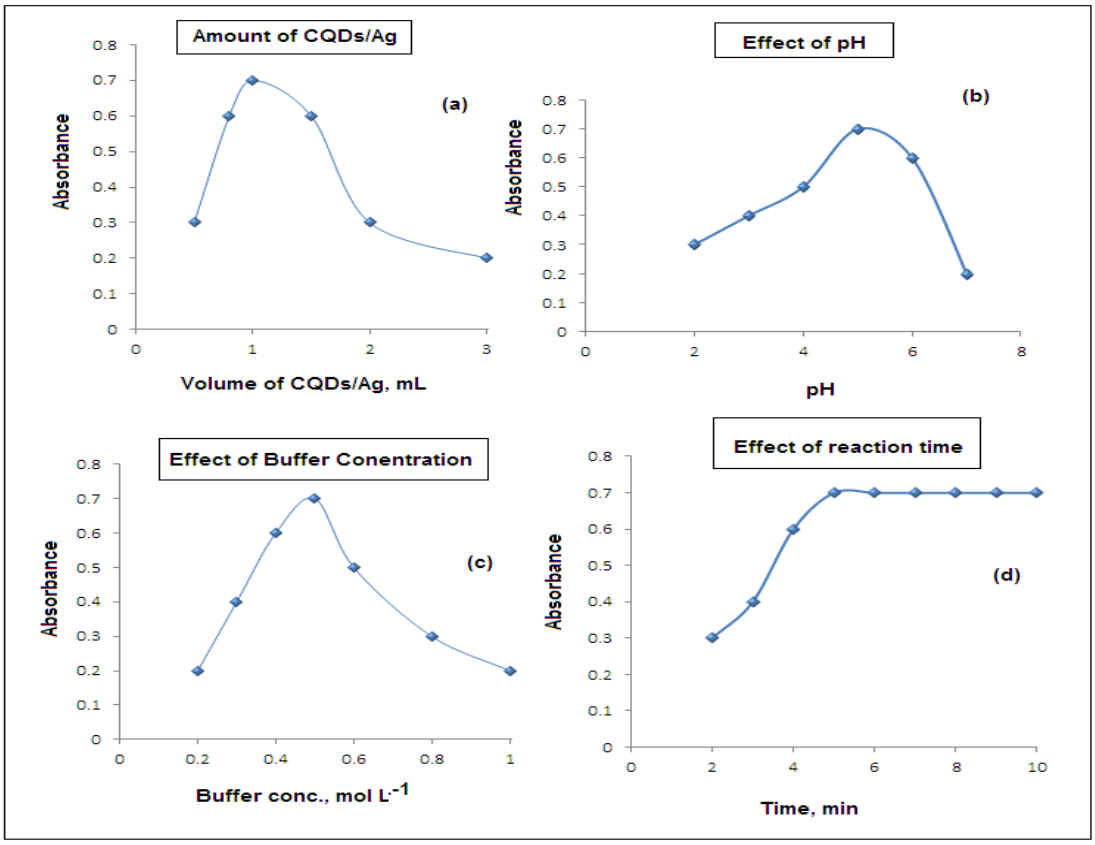

Figure 7: Optimization of conditions: (a) Effect of nanocomposite volume, (b) Effect of pH value, (c) Effect of buffer concentration, (d) Effect of reaction time.

Analytical figures of merit

After optimizing the analytical conditions, the proposed method was used for the detection of the investigated drug pure samples and the analytical figures of merit were obtained. The plotted calibration graph was linear over a concentration range of 5-80 µgmL^{-1} (Figure 8) and limit of detection 2.0 µgmL^{-1}. The regression equation was derived A = 0.0051C – 0.5836, (r = 0.9995) and relative standard deviation percentage (RSD %) of six replicate measurements equals 0.9 %. The obtained results revealed that the suggested method possessed a high sensitivity, good stability and acceptable linearity.

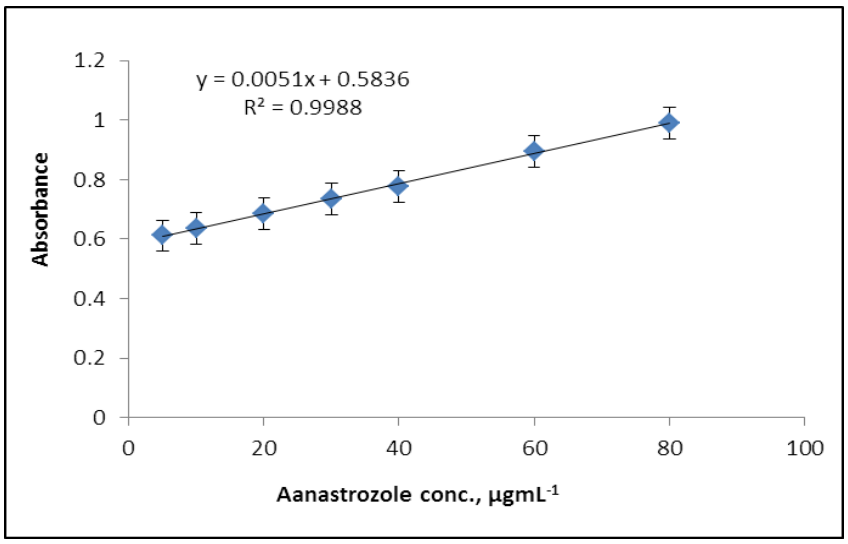

Figure 8: Calibration graph of ATZ detection using CDQs/Ag nanocomposite.

Method validation

Linearity

Under experimental conditions, the linearity of the proposed CQDs/Ag method was evaluated by analyzing a series of standard solutions (three replicates for each one) of ATZ and measured by following the procedure described in the experimental section. Table 1, resumed the obtained results from statistical analysis of data. The calibration graph was linear in the ranges of 5-80 µg mL^{-1}. The regression equation was A = 0.0051C – 0.5836, n=7 and (r = 0.9995).

Table 1: Analytical data obtained from the determination of ATZ using a spectrophotometric method in the presence of CQDs/Ag sensing solution.

Parameter	ATZ
Wavelength, nm	224
Linear concentration range, µg mL^{-1}	5-80
Regression equation	A = 0.0051C – 0.5836
Correlation coefficients, r	0.9995
LOD, µg mL^{-1}	2.0
LOQ, µg mL^{-1}	5.0
Accuracy	99.3±0.6

Limit of detection (LOD) and limit of quantitation (LOQ)

The suggested system displayed excellent sensitivity to the target analyte with LOD and LOQ of 2.0 and 5.0 µg mL^{-1}, respectively. The obtained analytical data revealed high sensitivity for ATZ detection.

Accuracy and precision

To prove the accuracy of the proposed method, the % recovery was determined over the concentration range of 5-80 µg mL^{-1} using CQDs/Ag nanocomposite sensing solution. The % recovery was found to be 99.3 ±0.6 %, revealing high accuracy of the suggested method (Table 2).

Table 2: The data obtained for the accuracy test using a spectrophotometric method in the presence of CQDs/Ag sensing solution.

Sample	ATZ detection using CQDs/Ag		
	Taken, µg mL^{-1}	Found, µg mL^{-1}	% Recovery
1	5	4.99	99.8
2	10	9.86	98.6
3	20	19.67	98.4
4	30	30.00	100.0
5	40	39.74	99.4
6	50	49.56	99.1
7	60	59.36	98.9
8	70	69.78	99.7
9	80	79.99	99.9
Mean±SD	99.3±0.6		
n	9		
Variance	0.36		
% SE	0.20		

Furthermore, to evaluate the precision of the proposed method, intra-day and inter-day precision were applied by determining three different concentrations of the investigated drug in pure form through three successive occasions or by replicating the analysis for a period of three successive days (Table 3). The evaluated % RSD ranged from 0.4-0.8 % for intra-day assay and 0.2-0.9 % for inter-day, indicating High precision of the suggested method towards the detection of ATZ.

Table 3: The data obtained for the evaluation of proposed method precision using intra-day and inter-day assay.

Sample	ATZ detection using CQDs/Ag			
	Taken, µg mL^{-1}	Found, µg mL^{-1}	% Recovery, (n=3)	% RSD
Intra-day assay	5	4.98	99.6±0.8	0.8
	40	39.99	99.9±0.4	0.4
	80	80.00	100.0±0.7	0.7
Inter-day assay	5	4.96	99.2±0.2	0.2
	40	39.87	99.7±0.9	0.9
	80	79.85	99.8±0.5	0.5

Selectivity

The selectivity of the proposed method towards the detection of ATZ was evaluated by assaying ATZ in the presence of some possible interfering species. Among these are Na^{+}, K^{+}, Ca^{2+}, Mg^{2+} and Zn^{2+}, starch, glucose, lactose, citric acid and magnesium stearate. Under optimized conditions the detection of 10 µg mL^{-1} of ATZ was investigated in the presence of 1.0 µg mL^{-1} of each interfering species using the proposed method. As reported in Table 4, no significant interference was observed. Accordingly, the proposed procedure can be considered as a selective method for the detection of ATZ.

Table 4: Tolerable limits of 10 µg mL^{-1} ATZ detection in the presence of some interferences using a a spectrophotometric method in the presence of CQDs/Ag nanocomposite.

Interferences	Tolerable values
Na^{+}, K^{+}, Ca^{2+}, Mg^{2+} and Zn^{2+}	800
Starch, glucose, lactose	350
Citric acid, magnesium stearate	200

Analysis of pharmaceutical preparation

The proposed CQDs/Ag nanocomposite was employed to detect ATZ in its pure drug and the % recovery was calculated as 99.7±0.4 % (Table 5). Also, the developed method was used to

estimate the ATZ in its pharmaceutical dosage form. The obtained data were assessed statistically and then compared with those obtained from other previously spectrophotometric published article[9] using t-student and F-test at 95% confidence level[27] (Table 6).

Table 5: Analytica data obtained by the detection of ATZ in pure form using the proposed method in the presence of CQDs/Ag nanocomposite.

Sample	ATZ detection using CQDs/Ag		
	Taken, µg mL^{-1}	Found, µg mL^{-1}	% Recovery
1	5	4.95	99.0
2	10	10.00	100.00
3	20	19.96	99.8
4	30	29.99	99.9
5	40	39.87	99.7
6	80	79.98	99.9
Mean±SD	99.7±0.4		
n	6		
Variance	0.16		
% SE	0.16		

Table 6: Analytica data obtained by the detection of ATZ in its tablets using the proposed method in the presence of CQDs/Ag nanocomposite.

Sample	ATZ detection using CQDs/Ag			
	Taken, µg mL^{-1}	Found, µg mL^{-1}	% Recovery	Reported method[9]
1	5	4.97	99.4	
2	10	9.93	99.3	
3	20	19.98	99.9	
4	30	29.87	99.7	
5	40	39.58	98.9	
6	80	79.95	99.9	
Mean±SD	99.5±0.4			99.2±0.6
n	6			6
Variance	0.16			0.36
% SE	0.16			0.24
t-test	1.040 (2.228)*			
F-test	2.25 (5.05)*			

CONCLUSION

A new spectrophotometric approach based on the use of a highly sensitive CQDs/Ag nanocomposite sensing solution has been developed for the detection of ATZ a breast cancer therapy in bulk and pharmaceutical formulations. The unique characteristics of CQDs which are mono-disperse, homogeneously distributed spherical particles and can emit green color

under UV light, provided a highly sensitive detecting solution for the investigated drug. The proposed technique displayed excellent results with linear concentrated rage of 5-80 µg mL^{-1}.

The obtained results indicated that this technique is simpler and more flexible to explore other sensing solution for the detection of different kinds of cancer therapy agents.

CONFLICT OF INTEREST

No conflict of interest associated with this work.

ACKNOWLEDGMENT

This research project was supported by a grant from the "Research center of the female Scientific and Medical Collages", Deanship of Scientific Research, King Saud University.

REFERENCES

1. Siegel R, Miller K, Jemal A, Cancer Statistics, Cancer J Clin, 2017; 67: 7-30.
2. Delivering on the Global Partnership for Achieving the Millennium Development Goals. New York, NY, United Nations, 2008.
3. Budavari S**,** The Merck Index an encyclopedia of chemicals, drugs and biologicals, 1996**.**
4. Ravisankar P, Rao GD, A novel validated RP-HPLC method for the determination of anastrozole in bulk and pharmaceutical tablet dosage forms. Der Pharm Chem, 2013; 5(3): 51-62.
5. Kumari MV, Eswaramma P, Kumar MS, Sreelatha M, Swapna R, Stability indicating analytical method validation of anastozole in pharmaceutical dosage form by RP-HPLC. Int J Innov Pharm Sci Res, 2015; 3(5): 493-503.
6. Abubakar MB, Gan SH, A Review of chromatographic methods used in the determination of anastrozole levels. Indian J Pharm Sci, 2016; 78(2): 173-181.
7. Duan G, Liang J, Zuo M, Rapid determination of anastrozole in plasma by gas chromatography with electron capture detection and its application to an oral pharmacokinetic study in healthy volunteers. Biomed Chromatogr, 2002; 16(6): 400-403.
8. Berzas JJ, Rodriguez J, Contenro AM, Cabello MP, Determination of drugs used in advanced breast cancer by capillary gas chromatography of pharmaceutical formulations. Sep Sci, 2003; 26(9-10): 908-914.
9. Banerjee M, Dash TK, Kumari A, Khatua S, Optimized UV-Vis spectrophotometric method for estimation of anastrozole in pharmaceutical solid dosage form. Der Pharm Chem, 2014; 6(3): 140-144.

10. Shin TH, Cheon J, Synergism of nanomaterials with physical stimuli for biology and medicine. Acc Chem Res, 2017**;** 50: 567-572.
11. Wang J, Gu H, Novel metal nanomaterials and their catalytic applications. Molecules, 2015; 20: 17070-17092.
12. Mallakpour S, Khadadazadeh L, Ultrasonic-assisted fabrication of starch/MWCNT-glucose nanocomposites for drug delivery. Ultrason Sonochem, 2018; 40: 401-409.
13. Taghdisi SM, Danesh NM, Ramezani M, Yazdian-Robati R, Abnous K, An amplified fluorescent aptasensor based on single-stranded DNA binding protein, copper and silica nanoparticles for sensitive detection of interferon-gamma. Anal Chem Acta, 2017; 984: 162-167.
14. Zhao H, Ding R, Zhao X, Li Y, Qu L, Pei H, Yildirimer L, Wu Z, Zhang W, Graphene-based nanomaterials for drug and/or gene delivery, bioimaging and tissue engineering. Dr Dis Today, 2017; 2: 1302-1317.
15. Ryvolova M, Chomoucka J, Drbohlavova J, Kopel P, Babula P, Hynek D, Adam V, Eckschlager T, Hubalek J, Stiborova M, Kaiser J, Kizek R, Modern micro and nanoparticle-based imaging techniques. Sensors, 2012; 12: 14792-14820.
16. Fernandez-Baldo MA, Oetega FG, Pareira SV, Bertolino FA, Serrano MJ, Lorente JA, Raba J, Messina GA, Nanostructured platform integrated into a microfluidic immunosensor coupled to laser-induced fluorescence for the epithelial cancer biomarker determination. Michrochem J, 2016; 128: 18-25.
17. Carlo GD, Curulli A, Toro RG, Bianchini C, De Caro T, Padeletti G, Zane D, Ingo GM, Green synthesis of gold-chitosan nanocomposites for caffeic acid sensing. Langmuir, 2012; 28: 5471-5479.
18. Yuan W, Gu Y, Li L, Green synthesis of graphene/Ag nanocomposites. Appl Sur Sci, 2012; 261: 753-758.
19. Shen L-M, Chen Q, Sun Z-Y, Chen X-W,Wang J-H, Assay of biothiols by regulating the growth of silver nanoparticles with C-dots as reducing agent. Anal Chem, 2014; 86: 5002-5008.
20. Samal M, Mohapatra P, Subbiah R, Lee CL, Anass B, Kim JA, Kim T, Yi DK, InP/ZnS-graphene oxide and reduced graphene oxide nanocomposites as fascinating materials for potential optoelectronic applications. Nanoscale, 2013; 5: 9793-97805.
21. Zhang Z, Zheng T, Li X, Xu J, Zeng H, Progress of carbon quantum dots in photocatalysis applications. Particle, 2016; 33: 457-472.

22. Javanbakht S, Namazi H, Solid state photoluminescence thermoplastic starch film containing graphene quantum dots. Carbohydr Polym, 2017; 176: 220-226.
23. Fan Z, Li S, Yuan F, Fan L, Fluorescent graphene quantum dots for biosensing and bioimaging. RSC Adv, 2015; 5: 19773-19789.
24. Choa YH, Yang JK, Kim BH, Jeong YK, Lee JS, Nakayama T et al. Preparation and characterization of metal: ceramic nanoporous nanocomposite powders. J Mag Mag Mat, 2003; 266(1-2): 12-19.
25. Yang Y, Liu Q, Cui J, Liu H, Wang P, Li Y, Chen L, Zhao Z, Dong Y, A novel label-free electrochemical immunosensor based on functionalized nitrogen-doped graphene quantum dots for carcinoembryonic antigen detection. Biosens. Bioelectron, 2017; 90: 31-38.
26. Chen S, Hai X, Chen X-W, Wang J-H, In situ growth of silver nanoparticles on graphene quantum dots for ultrasensitive colorimetric detection of H2O2 and glucose. Anal Chem, 2014; 86: 6689-6694.
27. Miller JC, Miller JN, Statistics for analytical chemistry. 3rd Ed. New York: Ellis Horwood PTR Prentice Hall, 1993.